A slender rivulet of a power-law fluid driven by either gravity or a constant shear stress at the free surface

S. K. Wilson*, B. R. Duffy† and R. Hunt‡

Department of Mathematics,
University of Strathclyde,
Livingstone Tower,
26 Richmond Street,
Glasgow G1 1XH,
United Kingdom

7th December 2000, revised 21st August and 31st October 2001

*Email : s.k.wilson@strath.ac.uk, Telephone : + 44 (0) 141 548 3820, Fax : + 44 (0) 141 552 8657

†Email : b.r.duffy@strath.ac.uk, Telephone : + 44 (0) 141 548 3645, Fax : + 44 (0) 141 552 8657

‡Email : r.hunt@strath.ac.uk, Telephone : + 44 (0) 141 548 3658, Fax : + 44 (0) 141 552 8657

Abstract

Similarity solutions that describe the flow of a slender non-uniform rivulet of non-Newtonian power-law fluid down an inclined plane are obtained. Rivulets driven by either gravity or a constant shear stress at the free surface are investigated, and in both cases solutions are obtained for both weak and strong surface-tension effects. We find that, despite the rather different physical mechanisms driving the flow, the solutions for gravity-driven and shear-stress-driven rivulets are qualitatively similar. When surface-tension effects are weak there is a unique similarity solution in which the transverse rivulet profile has a single global maximum. This solution represents both a diverging and thinning sessile rivulet and a converging and thickening pendent rivulet. On the other hand, when surface-tension effects are strong there is a one-parameter family of similarity solutions in which the transverse profile of a diverging and thinning rivulet has one global maximum, while that of a converging and thickening rivulet has either one global maximum or two equal global maxima. We also show how the present similarity solutions can be modified to accommodate a fixed-contact-angle condition at the contact line by incorporating sufficiently strong slip at the solid/fluid interface into the model.

1 Introduction

Rivulets occur in a wide variety of practical situations ranging from various geophysical flows to industrial devices such as condensers and heat exchangers. In many situations (such as, for example, many geophysical flows) gravity is the main driving force, while in others (such as, for example, an oil film on the wall of an aero-engine bearing chamber, ice accreting on an aircraft wing, or rain on the windscreen of a moving car) the surface shear and/or the pressure gradient due to an external airflow play a significant role. While some of the fluids encountered in practice are essentially Newtonian, many exhibit significantly non-Newtonian behaviour.

The pioneering analysis of the flow of a non-uniform rivulet of Newtonian fluid was performed by Smith [1] who obtained a similarity solution of the thin-film equation describing the steady gravity-driven draining of a slender non-uniform rivulet of Newtonian fluid from a point source on an inclined plane in the case of weak surface-tension effects. Smith's [1] solution predicts that the width of the rivulet increases or decreases like the 3/7th power of the distance measured down the plane from the source and that the height of the rivulet correspondingly decreases or increases like the $-1/7$th power, and is in good agreement with his own experimental measurements and with the numerically calculated solutions of the appropriate thin-film equation obtained by Schwartz and Michaelides [2]. Subsequently Duffy and Moffatt [3] performed the corresponding analysis in the case of strong surface-tension effects and, in particular, found that Smith's exponents are modified to 3/13th and $-1/13$th powers respectively. Recently Wilson, Duffy and Davis [4] obtained the corresponding similarity solutions for a slender dry patch in a fluid film draining under gravity down an inclined plane. All of these similarity solutions predict a varying contact angle at the contact line; Wilson, Duffy and Davis [4] showed that the rivulet similarity solutions of Smith [1] and Duffy and Moffatt [3] (but not, interestingly, their own dry-patch similarity solutions) can be modified to accommodate a fixed-contact-angle condition at the contact line by incorporating sufficiently strong slip at the solid/fluid interface into the model. Wilson and Burgess [6] generalised Smith's [1] similarity solution to flow of a power-law fluid. Coussot and Proust [5] derived the thin-film equation for a slender non-uniform rivulet of a Herschel-Bulkley material. This equation does not admit a similarity solution, but Coussot and Proust [5] did obtain a similarity solution to an approximate version of their equation which is in qualitative (but not quantitative) agreement with a series of their own experimental measurements made using various muds. Subsequently Wilson and Burgess [6] found that for the two experiments for which Coussot and Proust's [5] unapproximated equation is appropriate, numerically calculated solutions and the experimental measurements are in quantitative agreement.

Towell and Rothfeld [7] pioneered the investigation of the steady unidirectional flow of a uniform rivulet of Newtonian fluid down an inclined plane, and their approach was used by Rosenblat [8] to study uniform (but not unidirectional) flow of a viscoelastic fluid, and by Alekseenko, Geshev and Kuibin [9] to study unidirectional flow down the lower surface of an inclined circular cylinder. Duffy and Moffatt [10] used the lubrication

approximation employed by Allen and Biggin [11] to obtain analytically the leading-order solution for Newtonian rivulet flow down a planar substrate in the special case when the cross-sectional profile of the rivulet in the plane transverse to the flow is thin, and then interpreted their results as describing the locally unidirectional flow down a locally planar substrate whose local slope varies slowly in the flow-wise direction and, in particular, used them to describe the flow in the azimuthal direction round a large horizontal circular cylinder. Recently this approach has been extended to investigations of locally unidirectional flow down a substrate with variation transverse to the direction of flow by Wilson and Duffy [12], of locally uniform (but not locally unidirectional) flow down a uniformly heated or cooled substrate when thermocapillary effects are significant by Holland, Duffy and Wilson [13], and of locally unidirectional flow of a rivulet of viscoplastic material by Wilson, Duffy and Ross [14].

As far as the authors are aware there have been no analytical studies of shear-stress-driven rivulets; however there has been work on a variety of other thin-film flows in which the surface shear and/or the pressure gradient due to an external airflow play a significant role. For example, Moriarty, Schwartz and Tuck [15] considered the unsteady flow of a two-dimensional drop on a horizontal substrate spreading under the action of a jet of air blowing either vertically downward onto the drop (in which case the jet was modelled as a non-uniform pressure distribution) or horizontally over the drop (in which case it was modelled as a constant shear-stress distribution). King, Tuck and Vanden-Broeck [16] studied steady two-dimensional periodic waves on a fluid film on an inclined plane caused by a jet of air flowing upwards over it. Their model (which is based on thin-aerofoil theory) allows the external pressure gradient to depend on the shape of the free surface of the film, but assumes that the shear stress at the free surface is constant. King and Tuck [17] studied the corresponding problem for a ridge of fluid of finite width on an inclined plane. Myers and Thompson [18] formulated the general evolution equation for a three-dimensional fluid film driven by gravity, surface tension, external pressure gradient and surface-shear-stress effects, and described its steady two-dimensional solution in the special case of no external pressure gradient and a constant surface shear stress. McKinley, Wilson and Duffy [19] studied the quasi-static spreading of both a two-dimensional and an axisymmetric three-dimensional drop (either with or without a dry patch at its centre) due to a jet of air acting normally to the substrate; the jet of air was modelled as a parabolic pressure distribution, and sessile, pendent and zero-gravity situations were considered. Recently McKinley and Wilson [20, 21] investigated the linear stability of both two-dimensional and axisymmetric three-dimensional situations in the absence of gravity effects.

In this paper we follow the approach of Smith [1] and Duffy and Moffatt [3] and obtain similarity solutions that describe the flow of a slender non-uniform rivulet of non-Newtonian power-law fluid down an inclined plane. Rivulets driven by either gravity or a constant shear stress at the free surface are investigated, and in both cases solutions are obtained for both weak and strong surface-tension effects.

2 Problem Formulation

Consider the steady flow of a symmetric thin rivulet of a power-law fluid with uniform density ρ, constant surface tension σ, and variable viscosity $\mu = \mu_0 q^{N-1}$, where μ_0 is a constant, q is the local shear rate and $N > 0$ is the power-law index, on a planar substrate inclined at an angle α (where $0 \leq \alpha \leq \pi$) to the horizontal. When $0 < N < 1$ the fluid is shear thinning, when $N > 1$ it is shear thickening and when $N = 1$ the special case of a Newtonian fluid with constant viscosity μ_0 is recovered. Cartesian coordinates (x, y, z) with the x-axis down the line of greatest slope and the z-axis normal to the plane are adopted. We shall consider rivulets driven by either the x-component of gravity $g \sin\alpha$ or a constant shear stress T in the x-direction on the free surface. Since changing the sign of $g \sin\alpha$ or T simply corresponds to reversing the direction of the x-axis, we shall assume hereafter that $g \sin\alpha > 0$ or $T > 0$, as appropriate. The edges of the rivulet are at $y = \pm y_e(x)$. The geometry of the problem is shown in Figure 1. Making the familiar lubrication approximation the velocity (u, v, w), pressure p and free-surface position $z = h(x, y)$ satisfy the governing equations

$$u_x + v_y + w_z = 0, \tag{1}$$

$$(\mu u_z)_z - p_x + \rho g \sin\alpha = 0, \tag{2}$$

$$(\mu v_z)_z - p_y = 0, \tag{3}$$

$$-p_z - \rho g \cos\alpha = 0, \tag{4}$$

subject to the boundary conditions

$$u = v = w = 0 \tag{5}$$

on the substrate $z = 0$ and

$$p = -\sigma \nabla^2 h, \tag{6}$$

$$\mu u_z = T, \quad \mu v_z = 0 \tag{7}$$

on $z = h$, together with the kinematic condition on $z = h$, which can be written in the form

$$\nabla \cdot (\bar{u}, \bar{v}) = 0, \tag{8}$$

where

$$\bar{u} = \int_0^h u \, \mathrm{d}z, \quad \bar{v} = \int_0^h v \, \mathrm{d}z \tag{9}$$

are the local fluxes in the x and y directions respectively. If we write $P_x = p_x - \rho g \sin\alpha$, $s = T - P_x(h - z)$ and $s_0 = T - P_x h$ then integrating (2)–(4) subject to the boundary conditions (5)–(7) yields

$$u = \frac{\mu_0^{-\frac{1}{N}}}{P_x} \int_{s_0}^{s} \hat{s}\, \tau^{\frac{1-N}{N}} \, \mathrm{d}\hat{s}, \tag{10}$$

$$v = \frac{\mu_0^{-\frac{1}{N}} p_y}{P_x^2} \int_{s_0}^{s} (\hat{s} - T)\, \tau^{\frac{1-N}{N}}\, \mathrm{d}\hat{s}, \tag{11}$$

$$p = \rho g \cos\alpha (h - z) - \sigma \nabla^2 h, \tag{12}$$

where the scalar measure of the local stress, $\tau = \mu q$, is given by

$$\tau = \left[s^2 + \frac{p_y^2}{P_x^2} (T - s)^2 \right]^{\frac{1}{2}}, \tag{13}$$

and hence

$$\bar{u} = -\frac{\mu_0^{-\frac{1}{N}}}{P_x^2} \int_{s_0}^{T} \hat{s}\, (\hat{s} - T)\, \tau^{\frac{1-N}{N}}\, \mathrm{d}\hat{s}, \tag{14}$$

$$\bar{v} = -\frac{\mu_0^{-\frac{1}{N}}}{P_x^3} \int_{s_0}^{T} p_y\, (\hat{s} - T)^2\, \tau^{\frac{1-N}{N}}\, \mathrm{d}\hat{s}. \tag{15}$$

The kinematic condition (8) yields the governing partial differential equation for h. The prescribed constant total flux of fluid across any section $x =$ constant, denoted by Q, is given by

$$Q = \int_{-y_e}^{+y_e} \bar{u}\, \mathrm{d}y. \tag{16}$$

From now on we consider a slender rivulet that varies much more slowly in the x-direction than in the y-direction; for such a rivulet y-derivatives are much larger than x-derivatives, $P_x \simeq -\rho g \sin\alpha$, and $\tau \simeq \mu |u_z| = |s|$, and so at leading order (10)–(15) can be evaluated explicitly to yield

$$u = \frac{N \mu_0^{-\frac{1}{N}}}{(N+1)\rho g \sin\alpha} \left[|s_0|^{\frac{N+1}{N}} - |s|^{\frac{N+1}{N}} \right], \tag{17}$$

$$v = \frac{N \mu_0^{-\frac{1}{N}} p_y}{(\rho g \sin\alpha)^2} \left[\frac{|s|^{\frac{N+1}{N}} - |s_0|^{\frac{N+1}{N}}}{N+1} - T \left(s|s|^{\frac{1-N}{N}} - s_0 |s_0|^{\frac{1-N}{N}} \right) \right], \tag{18}$$

$$p = \rho g \cos\alpha (h - z) - \sigma h_{yy}, \tag{19}$$

$$\bar{u} = \frac{N \mu_0^{-\frac{1}{N}}}{(\rho g \sin\alpha)^2} \left[\frac{N T^{\frac{2N+1}{N}}}{(2N+1)(N+1)} + |s_0|^{\frac{N+1}{N}} \left(\frac{s_0}{2N+1} - \frac{T}{N+1} \right) \right], \tag{20}$$

$$\bar{v} = \frac{N \mu_0^{-\frac{1}{N}} p_y}{(\rho g \sin\alpha)^3} \left[\frac{2N^2 T^{\frac{2N+1}{N}}}{(2N+1)(N+1)} - s_0 |s_0|^{\frac{1-N}{N}} \left(\frac{s_0^2}{2N+1} - \frac{2T s_0}{N+1} + T^2 \right) \right]. \tag{21}$$

Setting $T = 0$ in (8) and (16) the governing equations for a slender gravity-driven rivulet are found to be

$$\left[h^{\frac{2N+1}{N}} (\rho g \cos\alpha h - \sigma h_{yy})_y \right]_y - \rho g \sin\alpha \left[h^{\frac{2N+1}{N}} \right]_x = 0 \tag{22}$$

and

$$Q = \frac{N}{2N+1}\left(\frac{\rho g \sin\alpha}{\mu_0}\right)^{\frac{1}{N}} \int_{-y_e}^{+y_e} h^{\frac{2N+1}{N}}\,\mathrm{d}y. \tag{23}$$

Note that in the special case $N = 1$ equations (22) and (23) reduce to the equations describing the flow of a gravity-driven Newtonian rivulet studied by Smith [1] and Duffy and Moffatt [3].

Taking the limit $g\sin\alpha \to 0$ in (8) and (16) the governing equations for a slender shear-stress-driven rivulet are found to be

$$\frac{1}{3}\left[h^3(\rho g\cos\alpha h - \sigma h_{yy})_y\right]_y - \frac{T}{2}\left[h^2\right]_x = 0 \tag{24}$$

and

$$Q = \frac{1}{2}\left(\frac{T}{\mu_0}\right)^{\frac{1}{N}} \int_{-y_e}^{+y_e} h^2\,\mathrm{d}y. \tag{25}$$

Note that (24) (but not (25)) is independent of N.

For both problems the governing equations are in the form

$$\frac{1}{3}\left[h^A(\rho g\cos\alpha h - \sigma h_{yy})_y\right]_y - \mathcal{F}\left[h^B\right]_x = 0 \tag{26}$$

and

$$Q = \mathcal{G}\int_{-y_e}^{+y_e} h^B\,\mathrm{d}y, \tag{27}$$

where in the gravity-driven case

$$A = B = \frac{2N+1}{N}, \quad \mathcal{F} = \frac{\rho g\sin\alpha}{3}, \quad \mathcal{G} = \frac{N}{2N+1}\left(\frac{\rho g\sin\alpha}{\mu_0}\right)^{\frac{1}{N}}, \tag{28}$$

while in the shear-stress-driven case

$$A = 3, \quad B = 2, \quad \mathcal{F} = \frac{T}{2}, \quad \mathcal{G} = \frac{1}{2}\left(\frac{T}{\mu_0}\right)^{\frac{1}{N}}. \tag{29}$$

Here we shall consider only rivulets that are symmetric about $y = 0$, and impose the regularity conditions

$$h_y = h_{yyy} = 0 \tag{30}$$

at $y = 0$; in addition h satisfies the contact-line condition

$$h = 0 \tag{31}$$

at $y = y_e$. We might also wish to impose a fixed-contact-angle condition in the form $h_y = -\theta$ at $y = y_e$, where θ is a (small) prescribed constant contact angle. However, as we shall see, the similarity solutions derived in sections 3 and 4 cannot, in general, satisfy a condition of this form. In section 5 we show how these similarity solutions can

be modified in a small region near to the contact line in order to accommodate such a condition.

For both problems we shall consider both the case of weak surface-tension effects in which the typical transverse lengthscale (i.e. in the y-direction) is much greater than $(\sigma/\rho g|\cos\alpha|)^{1/2}$ so that gravity dominates surface tension in the pressure (as studied by Smith [1] for a gravity-driven Newtonian rivulet), and the case of strong surface-tension effects in which the typical transverse lengthscale is much less than $(\sigma/\rho g|\cos\alpha|)^{1/2}$ so that surface tension dominates gravity in the pressure (as studied by Duffy and Moffatt [3] for a gravity-driven Newtonian rivulet). Specifically, for weak surface-tension effects equations (26) and (27) with the surface-tension term σh_{yy} neglected are valid provided that the appropriately defined longitudinal and transverse aspect ratios (that is, in the x-y and y-z planes respectively) are sufficiently small:

$$\left[\left(\frac{Q}{\mathcal{G}}\right)^{A-B+1}\left(\frac{\rho g|\cos\alpha|}{\mathcal{F}}\right)^{B} l^{-(A+1)}\right]^{\frac{1}{A+B+1}} \ll 1, \tag{32}$$

$$\left[\left(\frac{Q}{\mathcal{G}}\right)^{B-A+1}\left(\frac{\mathcal{F}}{\rho g|\cos\alpha|\, l}\right)^{B+1}\right]^{\frac{1}{A+B+1}} \ll 1, \tag{33}$$

and provided that the transverse lengthscale is sufficiently large:

$$\left[\left(\frac{Q}{\mathcal{G}}\right)^{A-B+1}\left(\frac{\rho g|\cos\alpha|\, l}{\mathcal{F}}\right)^{B}\right]^{\frac{1}{A+B+1}} \gg \left(\frac{\sigma}{\rho g|\cos\alpha|}\right)^{\frac{1}{2}}, \tag{34}$$

where l denotes a typical longitudinal lengthscale (i.e. in the x-direction). For strong surface-tension effects equations (26) and (27) with the gravity term $\rho g\cos\alpha h$ neglected are again valid provided that the relevant aspect ratios are sufficiently small:

$$\left[\left(\frac{Q}{\mathcal{G}}\right)^{A-B+1}\left(\frac{\sigma}{\mathcal{F}}\right)^{B} l^{-(A+2B+1)}\right]^{\frac{1}{A+3B+1}} \ll 1, \tag{35}$$

$$\left[\left(\frac{Q}{\mathcal{G}}\right)^{B-A+3}\left(\frac{\mathcal{F}}{\sigma l}\right)^{B+1}\right]^{\frac{1}{A+3B+1}} \ll 1, \tag{36}$$

and provided that the transverse lengthscale is sufficiently small:

$$\left[\left(\frac{Q}{\mathcal{G}}\right)^{A-B+1}\left(\frac{\sigma l}{\mathcal{F}}\right)^{B}\right]^{\frac{1}{A+3B+1}} \ll \left(\frac{\sigma}{\rho g|\cos\alpha|}\right)^{\frac{1}{2}}. \tag{37}$$

For both problems we seek a similarity solution for h in the form

$$h = b(cx)^m G(\eta), \quad \text{where} \quad \eta = \frac{y}{y_e(x)} \quad \text{and} \quad y_e = (cx)^n, \tag{38}$$

in which the constants b, c, m and n are to be determined, and in which G satisfies the regularity conditions

$$G'(0) = G'''(0) = 0, \tag{39}$$

and the contact-line condition

$$G(1) = 0. \tag{40}$$

Evidently we must have $y_e \geq 0$ and $h \geq 0$ for this solution to be physically relevant. We shall consider only solutions for which $cx \geq 0$, and since we shall find that $m < 0$ and $0 < n < 1$ in all the cases considered in the present work this means that solutions for $c > 0$ represent diverging and thinning rivulets in $x > 0$ and solutions for $c < 0$ represent converging and thickening rivulets in $x < 0$. Furthermore, since we will always be able to choose $b > 0$ only solutions with $G \geq 0$ everywhere on the interval $[0, 1]$ are physically relevant.

3 General Solution for Weak Surface Tension

When surface-tension effects are weak the terms $[h^A h_y]_y$ and $[h^B]_x$ in (26) balance provided that $(A - B + 1)m = 2n - 1$, and the flux Q in (27) is independent of x provided that $Bm + n = 0$, and so

$$m = -\frac{1}{A + B + 1}, \quad n = \frac{B}{A + B + 1}. \tag{41}$$

If we choose

$$b = \left(\frac{3n\mathcal{F}}{\rho g}\left|\frac{c}{\cos\alpha}\right|\right)^{\frac{1}{A-B+1}} \tag{42}$$

then the governing equation for G is

$$\left[G^A G' + S\eta G^B\right]' = 0, \tag{43}$$

where

$$S = \operatorname{sgn}\left(\frac{c}{\cos\alpha}\right), \tag{44}$$

which can be integrated twice subject to (39) and (40) to yield

$$G = \left[\frac{S(A - B + 1)}{2}(1 - \eta^2)\right]^{\frac{1}{A-B+1}}. \tag{45}$$

For both of the problems considered here we shall find that real and positive solutions for G are possible only when $S = 1$, which means that c and $\cos\alpha$ must have the same sign and hence that solutions with $c > 0$ correspond to sessile rivulets and those with $c < 0$ to pendent rivulets. The flux is given by

$$Q = \mathcal{G}\int_{-1}^{+1} (bG)^B \, \mathrm{d}\eta, \tag{46}$$

so that

$$Q = \mathcal{G}I\left(\frac{3B\mathcal{F}}{\rho g(A+B+1)}\left|\frac{c}{\cos\alpha}\right|\right)^{\frac{B}{A-B+1}}, \tag{47}$$

where

$$I = \int_{-1}^{+1} G^B \,\mathrm{d}\eta = \int_{-1}^{+1}\left[\frac{S(A-B+1)}{2}(1-\eta^2)\right]^{\frac{B}{A-B+1}} \mathrm{d}\eta, \tag{48}$$

and hence c is given by

$$|c| = \frac{\rho g(A+B+1)|\cos\alpha|}{3B\mathcal{F}}\left(\frac{Q}{\mathcal{G}I}\right)^{\frac{A-B+1}{B}}. \tag{49}$$

3.1 Gravity-Driven Rivulet

This is the case investigated by Wilson and Burgess [6]. In this case $A = B = (2N+1)/N$ and so

$$m = -\frac{N}{5N+2}, \quad n = \frac{2N+1}{5N+2}. \tag{50}$$

Note that, as Wilson and Burgess [6] pointed out, neither m nor n change a great deal as N is varied. Specifically, m varies monotonically between 0 in the limit $N \to 0$ and $-1/5$ in the limit $N \to \infty$ taking the value $-1/7$ at $N = 1$, while n varies monotonically between $1/2$ in the limit $N \to 0$ and $2/5$ in the limit $N \to \infty$ taking the value $3/7$ at $N = 1$. A real and positive solution for G is possible only if $S = 1$, in which case

$$b = \frac{2N+1}{5N+2}c\tan\alpha \tag{51}$$

and

$$G = \frac{1}{2}(1-\eta^2), \tag{52}$$

so that $G(0) = 1/2$ and $G'(1) = -1$. Thus

$$Q = \frac{NI}{2N+1}\left(\frac{\rho g\sin\alpha}{\mu_0}\right)^{\frac{1}{N}}\left[\frac{2N+1}{5N+2}c\tan\alpha\right]^{\frac{2N+1}{N}}, \tag{53}$$

where

$$I = \int_{-1}^{+1}\left[\frac{1}{2}(1-\eta^2)\right]^{\frac{2N+1}{N}}\mathrm{d}\eta = \left(\frac{1}{2}\right)^{\frac{2N+1}{N}}\frac{\sqrt{\pi}\,\Gamma\left(\frac{3N+1}{N}\right)}{\Gamma\left(\frac{7N+2}{2N}\right)}, \tag{54}$$

and so

$$c = \frac{5N+2}{2N+1}\cot\alpha\left(\frac{\mu_0}{\rho g\sin\alpha}\right)^{\frac{1}{2N+1}}\left(\frac{(2N+1)Q}{NI}\right)^{\frac{N}{2N+1}}. \tag{55}$$

Note that Wilson and Burgess [6] did not evaluate I explicitly and that their version of (55) contains a typographical error. Figure 2 shows $I = I(N)$ given by (54) plotted as a function of N. As Fig. 2 shows, I is a monotonically increasing function of N satisfying

$$I \sim \left(\frac{1}{2}\right)^{\frac{2N+1}{N}} \sqrt{\pi N} \to 0 \tag{56}$$

as $N \to 0$, $I = 4/35$ when $N = 1$, and $I \to 4/15$ as $N \to \infty$. Hence

$$c \to \frac{4\mu_0 \cot\alpha}{\rho g \sin\alpha} \tag{57}$$

(which is independent of Q) in the strongly shear-thinning limit $N \to 0$,

$$c = \frac{7\cot\alpha}{3}\left(\frac{105\mu_0 Q}{4\rho g \sin\alpha}\right)^{\frac{1}{3}} \tag{58}$$

when $N = 1$, and

$$c \to \frac{5\cot\alpha}{2}\left(\frac{15Q}{2}\right)^{\frac{1}{2}} \tag{59}$$

(which is independent of ρ, g and μ_0) in the strongly shear-thickening limit $N \to \infty$.

Note that from (32)–(34) this solution is appropriate provided that

$$\left(\frac{\mu_0 Q^N}{\rho g \sin\alpha |\tan\alpha|^{2N+1} l^{3N+1}}\right)^{\frac{1}{5N+2}} \ll 1, \tag{60}$$

$$\left(\frac{\mu_0 Q^N |\tan\alpha|^{3N+1}}{\rho g \sin\alpha\, l^{3N+1}}\right)^{\frac{1}{5N+2}} \ll 1, \tag{61}$$

$$\left(\frac{\mu_0 Q^N l^{2N+1}}{\rho g \sin\alpha |\tan\alpha|^{2N+1}}\right)^{\frac{1}{5N+2}} \gg \left(\frac{\sigma}{\rho g |\cos\alpha|}\right)^{\frac{1}{2}}. \tag{62}$$

In the special case $N = 1$ we recover results equivalent to those of Smith [1] for a Newtonian rivulet.

3.2 Shear-Stress-Driven Rivulet

In this case $A = 3$ and $B = 2$ and so $m = -1/6$ and $n = 1/3$. Again a real and positive solution for G is possible only if $S = 1$, in which case

$$b = \left(\frac{cT}{2\rho g \cos\alpha}\right)^{\frac{1}{2}} \tag{63}$$

and

$$G = (1 - \eta^2)^{\frac{1}{2}}, \tag{64}$$

so that $G(0) = 1$ and $G'(1) = -\infty$. Thus

$$Q = \left(\frac{T}{\mu_0}\right)^{\frac{1}{N}} \frac{cT}{3\rho g \cos\alpha}, \tag{65}$$

where we have made use of the fact that

$$I = \int_{-1}^{+1} (1 - \eta^2)\, \mathrm{d}\eta = \frac{4}{3}, \tag{66}$$

and so

$$c = \left(\frac{\mu_0}{T}\right)^{\frac{1}{N}} \frac{3Q\rho g \cos\alpha}{T}. \tag{67}$$

Note that from (32)–(34) this solution is appropriate provided that

$$\left[\frac{Q\rho g|\cos\alpha|}{Tl^2}\left(\frac{\mu_0}{T}\right)^{\frac{1}{N}}\right]^{\frac{1}{3}} \ll 1, \tag{68}$$

$$\left(\frac{T}{\rho g|\cos\alpha|\, l}\right)^{\frac{1}{2}} \ll 1, \tag{69}$$

$$\left[\frac{Q\rho g|\cos\alpha|\, l}{T}\left(\frac{\mu_0}{T}\right)^{\frac{1}{N}}\right]^{\frac{1}{3}} \gg \left(\frac{\sigma}{\rho g|\cos\alpha|}\right)^{\frac{1}{2}}. \tag{70}$$

In the special case $N = 1$ we obtain new results for a Newtonian rivulet.

4 General Solution for Strong Surface Tension

When surface-tension effects are strong the terms $[h^A h_{yyy}]_y$ and $[h^B]_x$ in (26) balance provided that $m(A - B + 1) = 4n - 1$, and the flux Q in (27) is again independent of x provided that $Bm + n = 0$, and so

$$m = -\frac{1}{A + 3B + 1}, \quad n = \frac{B}{A + 3B + 1}. \tag{71}$$

If we choose

$$b = \left(\frac{3n|c|\mathcal{F}}{\sigma}\right)^{\frac{1}{A-B+1}} \tag{72}$$

then the governing equation for G is

$$\left[G^A G''' - S\eta G^B\right]' = 0, \tag{73}$$

where

$$S = \mathrm{sgn}(c), \tag{74}$$

which can be integrated once subject to (39) to yield the third-order equation

$$G^{A-B}G''' - S\eta = 0. \tag{75}$$

The flux is again given by (46) so that

$$Q = \mathcal{G}I\left(\frac{3n|c|\mathcal{F}}{\sigma}\right)^{\frac{B}{A-B+1}}, \tag{76}$$

where

$$I = \int_{-1}^{+1} G^B \, \mathrm{d}\eta, \tag{77}$$

and hence c is given by

$$|c| = \frac{\sigma}{3n\mathcal{F}}\left(\frac{Q}{\mathcal{G}I}\right)^{\frac{A-B+1}{B}}. \tag{78}$$

Unlike in the case of weak surface tension we cannot, in general, obtain the solution of the governing equation (75) for G in closed form. However, a straightforward Taylor expansion about $\eta = 0$ where $G = G(0) = G_0$ reveals that

$$G = G_0\left[1 + C_1\eta^2 + C_2\eta^4 + C_3\eta^6 + O(\eta^8)\right], \tag{79}$$

where the constant C_1 is undetermined locally and the constants C_2 and C_3 are given by

$$C_2 = \frac{S}{24G_0^{A-B+1}}, \quad C_3 = \frac{S(B-A)C_1}{120G_0^{A-B+1}}. \tag{80}$$

4.1 Gravity-Driven Rivulet

In this case $A = B = (2N+1)/N$ and so

$$m = -\frac{N}{9N+4}, \quad n = \frac{2N+1}{9N+4}. \tag{81}$$

Note that, as in the case of weak surface tension, neither m nor n change a great deal as N is varied. Specifically, m varies monotonically between 0 in the limit $N \to 0$ and $-1/9$ in the limit $N \to \infty$ taking the value $-1/13$ at $N = 1$, while n varies monotonically between $1/4$ in the limit $N \to 0$ and $2/9$ in the limit $N \to \infty$ taking the value $3/13$ at $N = 1$. We have

$$b = \frac{2N+1}{9N+4}\frac{|c|\rho g \sin\alpha}{\sigma} \tag{82}$$

and the governing equation for G is

$$G''' - S\eta = 0, \tag{83}$$

which can be solved exactly subject to (39), (40) and $G(0) = G_0$ to yield

$$G = (1-\eta^2)\left(G_0 - \frac{S\eta^2}{24}\right). \tag{84}$$

Thus

$$Q = \frac{NI}{2N+1}\left(\frac{\rho g \sin\alpha}{\mu_0}\right)^{\frac{1}{N}}\left(\frac{2N+1}{9N+4}\frac{|c|\rho g\sin\alpha}{\sigma}\right)^{\frac{2N+1}{N}}, \tag{85}$$

where

$$I = \int_{-1}^{+1}\left[(1-\eta^2)\left(G_0 - \frac{S\eta^2}{24}\right)\right]^{\frac{2N+1}{N}} \mathrm{d}\eta, \tag{86}$$

and so

$$|c| = \frac{9N+4}{2N+1}\frac{\sigma}{\rho g\sin\alpha}\left(\frac{\mu_0}{\rho g\sin\alpha}\right)^{\frac{1}{2N+1}}\left(\frac{(2N+1)Q}{NI}\right)^{\frac{N}{2N+1}}. \tag{87}$$

Figure 3 shows G given by (84) for a range of values of G_0. As Fig. 3 shows, when $S = 1$, G is non-negative everywhere on $[0,1]$ only if $G_0 \geq G_{0c} = 1/24$ and always has a single maximum at $\eta = 0$, whereas when $S = -1$, G is non-negative everywhere on $[0,1]$ for all $G_0 \geq 0$ and has a local maximum at $\eta = 0$ when $G_0 \geq G_0^* = 1/24$, and a local minimum at $\eta = 0$ together with two equal global maxima $G = G_{\mathrm{m}}(G_0)$ at $\eta = \pm\eta_{\mathrm{m}}(G_0)$, where

$$G_{\mathrm{m}} = \frac{(1+24G_0)^2}{96} \quad \text{and} \quad \eta_{\mathrm{m}} = \left[\frac{1-24G_0}{2}\right]^{\frac{1}{2}}, \tag{88}$$

when $G_0 < G_0^*$. The local behaviour of G as $\eta \to 1^-$ is

$$G = \left(2G_0 - \frac{S}{12}\right)(1-\eta) + O(1-\eta)^2. \tag{89}$$

Figure 4(a) shows $I = I(G_0, N)$ given by (86) plotted as a function of G_0 for a range of values of N for both $S = 1$ and $S = -1$, while Fig. 4(b) shows I plotted as a function of N for a range of values of G_0 for both $S = 1$ and $S = -1$. As Fig. 4 shows, for physically acceptable values of G_0 the integral I is a monotonically increasing function of G_0 (but not N) satisfying

$$I \sim \begin{cases} 2G_0^{\frac{5N+2}{2N}}\left[\dfrac{6\pi N}{S+24G_0}\right]^{\frac{1}{2}} & \text{when } S = 1 \text{ or } S = -1 \text{ and } G_0 > G_0^*, \\ \dfrac{1}{2}\left(\dfrac{1}{24}\right)^{\frac{2N+1}{N}} N^{\frac{1}{4}}\Gamma\left(\tfrac{1}{4}\right) & \text{when } S = -1 \text{ and } G_0 = G_0^*, \\ 4G_{\mathrm{m}}^{\frac{5N+2}{2N}}\left[\dfrac{3\pi N}{1-24G_0}\right]^{\frac{1}{2}} & \text{when } S = -1 \text{ and } G_0 < G_0^* \end{cases} \tag{90}$$

(the Appendix gives details of how these expressions are derived) so that $I \to \infty$ when $G_0 > 1$ and $I \to 0$ when $G_0 \leq 1$ as $N \to 0$,

$$I = \frac{32}{35}G_0^3 - \frac{4S}{315}G_0^2 + \frac{1}{6930}G_0 - \frac{S}{1297296} \tag{91}$$

at $N = 1$,

$$I \to \frac{16}{15}G_0^2 - \frac{4S}{315}G_0 + \frac{1}{11340} \tag{92}$$

as $N \to \infty$, and

$$I \sim \frac{\sqrt{\pi}\,\Gamma\left(\frac{3N+1}{N}\right)}{\Gamma\left(\frac{7N+2}{2N}\right)}G_0^{\frac{2N+1}{N}} \tag{93}$$

as $G_0 \to \infty$. Hence

$$|c| \to \frac{4\mu_0\sigma}{(\rho g \sin\alpha)^2}\begin{cases} G_0^{-1} & \text{when } S = 1 \text{ or } S = -1 \text{ and } G_0 \geq G_0^*, \\ G_{\mathrm{m}}^{-1} & \text{when } S = -1 \text{ and } G_0 < G_0^* \end{cases} \tag{94}$$

(which is independent of Q) in the strongly shear-thinning limit $N \to 0$,

$$|c| = \frac{13\sigma}{3\rho g \sin\alpha}\left(\frac{3\mu_0 Q}{\rho g \sin\alpha I}\right)^{\frac{1}{3}} \tag{95}$$

where I is given by (91) at $N = 1$,

$$|c| \to \frac{9\sigma}{\rho g \sin\alpha}\left(\frac{Q}{2I}\right)^{\frac{1}{2}} \tag{96}$$

where I is given by (92) (which is independent of μ_0) in the strongly shear-thickening limit $N \to \infty$, and $|c| = O(G_0^{-1})$ as $G_0 \to \infty$.

Note that from (35)–(37) this solution is appropriate provided that

$$\left[\frac{\mu_0 Q^N \sigma^{2N+1}}{(\rho g \sin\alpha)^{2N+2} l^{7N+3}}\right]^{\frac{1}{9N+4}} \ll 1, \tag{97}$$

$$\left[\frac{\mu_0^3 Q^{3N}(\rho g \sin\alpha)^{3N-2}}{(\sigma l)^{3N+1}}\right]^{\frac{1}{9N+4}} \ll 1, \tag{98}$$

$$\left[\frac{\mu_0 Q^N (\sigma l)^{2N+1}}{(\rho g \sin\alpha)^{2N+2}}\right]^{\frac{1}{9N+4}} \ll \left(\frac{\sigma}{\rho g|\cos\alpha|}\right)^{\frac{1}{2}}. \tag{99}$$

In the special case $N = 1$ we recover results equivalent to those of Duffy and Moffatt [3] for a Newtonian rivulet.

4.2 Shear-Stress-Driven Rivulet

In this case $A = 3$ and $B = 2$ and so $m = -1/10$ and $n = 1/5$. We have

$$b = \left(\frac{3|c|T}{10\sigma}\right)^{\frac{1}{2}} \tag{100}$$

and the governing equation for G is

$$GG''' - S\eta = 0. \tag{101}$$

Thus

$$Q = \left(\frac{T}{\mu_0}\right)^{\frac{1}{N}} \frac{3|c|IT}{20\sigma}, \tag{102}$$

where

$$I = \int_{-1}^{+1} G^2 \, \mathrm{d}\eta, \tag{103}$$

and so

$$|c| = \left(\frac{\mu_0}{T}\right)^{\frac{1}{N}} \frac{20\sigma Q}{3IT}. \tag{104}$$

Unlike in the gravity-driven case, we cannot obtain the solution of the governing equation for G in closed form in this case. Therefore (101) was solved numerically for G subject to (39), (40) and $G(0) = G_0$ using pseudospectral differencing with Gauss-Lobatto points. Because of the logarithmically singular behaviour of G'' as $\eta \to 1^-$ (see below) as many as 100 points were required to obtain numerical results accurate to 6 decimal places. Figure 5 shows numerically calculated solutions for G for a range of values of G_0. In particular, Fig. 5 shows that the qualitative behaviour of G as G_0 is varied is the same as in the gravity-driven case, namely when $S = 1$, G is non-negative everywhere on $[0, 1]$ only if $G_0 \geq G_{0c} \simeq 0.4277$ and always has a single maximum at $\eta = 0$, whereas when $S = -1$, G is non-negative everywhere on $[0, 1]$ for all $G_0 \geq 0$ and has a local maximum at $\eta = 0$ when $G_0 \geq G_0^* \simeq 0.2138$ and a local minimum at $\eta = 0$ together with two equal global maxima $G = G_{\mathrm{m}}(G_0)$ at $\eta = \pm\eta_{\mathrm{m}}(G_0)$ when $G_0 < G_0^*$. A local analysis near $\eta = 1$ reveals that the local behaviour of G as $\eta = 1 - \xi \to 1^-$ (i.e. $\xi \to 0^+$) is either

$$G = A_0\xi + (A_1 + B_1 \log\xi)\xi^2 + (A_2 + B_2 \log\xi)\xi^3 + o(\xi^3), \tag{105}$$

where the constants B_1, A_2 and B_2 are given by

$$B_1 = -\frac{S}{2A_0}, \quad A_2 = \frac{1}{6A_0^3}\left[SA_0(A_0 + A_1) + \frac{11}{12}\right], \quad B_2 = -\frac{1}{12A_0^3}, \tag{106}$$

but the constants $A_0 > 0$ and A_1 are undetermined locally, or if $S = 1$

$$G = \left(\frac{8}{3}\right)^{\frac{1}{2}} \xi^{\frac{3}{2}} + \left(\frac{1}{6}\right)^{\frac{1}{2}} \xi^{\frac{5}{2}} - \frac{5}{204}\left(\frac{3}{8}\right)^{\frac{1}{2}} \xi^{\frac{7}{2}} + O\left(\xi^{\frac{9}{2}}\right). \tag{107}$$

Note that there is no solution satisfying $G'(1) = 0$ analogous to (107) when $S = -1$. The local behaviour of G near $\eta = 0$ is given by (79), where from (80)

$$C_2 = \frac{S}{24G_0^2}, \quad C_3 = -\frac{SC_1}{120G_0^2}. \tag{108}$$

Figure 6 shows $I = I(G_0)$ given by (103) plotted as a function of G_0 for both $S = 1$ and $S = -1$. As Fig. 6 shows, I satisfies $I \simeq 0.0163$ at $G_0 = 0$ when $S = -1$, $I \simeq 0.1731$ at $G_0 = G_{0c}$ when $S = 1$, and $I \sim 16G_0^2/15$ as $G_0 \to \infty$. Hence

$$|c| \sim \left(\frac{\mu_0}{T}\right)^{\frac{1}{N}} \frac{25\sigma Q}{4TG_0^2} \tag{109}$$

as $G_0 \to \infty$.

Note that from (35)–(37) this solution is appropriate provided that

$$\left[\frac{\sigma Q}{Tl^4}\left(\frac{\mu_0}{T}\right)^{\frac{1}{N}}\right]^{\frac{1}{5}} \ll 1, \tag{110}$$

$$\left[\frac{Q^2T^3}{(\sigma l)^3}\left(\frac{\mu_0}{T}\right)^{\frac{2}{N}}\right]^{\frac{1}{10}} \ll 1, \tag{111}$$

$$\left[\frac{\sigma Ql}{T}\left(\frac{\mu_0}{T}\right)^{\frac{1}{N}}\right]^{\frac{1}{5}} \ll \left(\frac{\sigma}{\rho g|\cos\alpha|}\right)^{\frac{1}{2}}. \tag{112}$$

In the special case $N = 1$ we obtain new results for a Newtonian rivulet.

5 Imposing a Fixed-Contact-Angle Condition at the Contact Line

Evidently the form of the present similarity solutions in which $h_y = b(cx)^{m-n}G'(\eta)$ is, in general, incompatible with a fixed-contact-angle condition. Wilson, Duffy and Davis [4] showed that the similarity solutions of Smith [1] and Duffy and Moffatt [3] for a gravity-driven Newtonian rivulet can be modified to accommodate the non-self-similar fixed-contact angle condition $h_y = -\theta$ at $\eta = 1$, where θ is a (small) prescribed constant contact angle, by incorporating sufficiently strong slip at the substrate into the model. In this section we show how the present solutions for both gravity-driven and shear-stress-driven rivulets of a power-law fluid can be modified in a similar way.

Following the approach of Wilson, Duffy and Davis [4] we replace the no-slip and no-penetration boundary conditions (5) at the substrate $z = 0$ by the slip and no-penetration conditions

$$u = \frac{\beta}{3}u_z, \quad v = \frac{\beta}{3}v_z, \quad w = 0 \tag{113}$$

at $z = 0$, where $\beta = \beta(h)$ is the (small) slip length. With these new boundary conditions (26) becomes

$$\frac{1}{3}\left[h^{A-1}(h+\lambda_1\beta)(\rho g\cos\alpha h - \sigma h_{yy})_y\right]_y - \mathcal{F}\left[h^{B-1}(h+\lambda_2\beta)\right]_x = 0, \tag{114}$$

where in the gravity-driven case

$$\lambda_1 = \lambda_2 = \frac{2N+1}{3N} \tag{115}$$

and A, B and $\mathcal{F}$ are again given by (28), while in the shear-stress-driven case

$$\lambda_1 = 1, \quad \lambda_2 = \frac{2}{3} \tag{116}$$

and A, B and $\mathcal{F}$ are again given by (29). Various models have been proposed for β; here we consider the fairly general form $\beta = \epsilon^{M+1}/h^M$, where ϵ is the small constant slip length and the slip-law exponent $M \geq 0$. The cases $M = 0$ and $M = 1$ recover the familiar models $\beta = \epsilon$ and $\beta = \epsilon^2/h$ used, for example, by Hocking [22] and Greenspan [23], respectively.

Slip is significant only in a small region of size $O(\epsilon)$ near the contact line in which $h_y = O(1)$. In this inner region we introduce appropriately rescaled inner variables Y and $H = H(x, Y)$ defined by

$$y = (cx)^n - \epsilon Y, \quad h = \epsilon H. \tag{117}$$

Provided that $B - A + 2 > 0$ (as it is for both of the problems considered here) at leading order in ϵ, equation (114) becomes simply

$$H^{A-1}(H + \lambda_1 H^{-M})H_{YYY} = K, \tag{118}$$

where $K = K(x)$ is an unknown function of x only. In the limit $H \to 0^+$ equation (118) becomes $\lambda_1 H_{YYY} = KH^{M-A+1}$ and so will permit a solution in the form $H = \theta Y + o(Y)$ as $Y \to 0^+$ only if $M > A - 3$, i.e. only if the slip is sufficiently strong. In the limit $H \to \infty$ equation (118) becomes $H_{YYY} = KH^{-A}$, which has a solution of the form $H = \phi Y + o(Y)$ as $Y \to \infty$, where $\phi = \phi(x)$ is an unknown function of x only, only if $A > 2$ (as it is for both of the problems considered here).

When surface-tension effects are strong the outer limit of the inner solution matches directly with the inner limit of the outer solution provided that $\phi = -b(cx)^{m-n}G'(1)$.

Even when surface-tension effects are weak they are always significant in a small region of size $O(\delta)$ near the contact line, where $\delta = (\sigma/\rho g\cos\alpha)^{1/2} \gg \epsilon$. In this intermediate region we introduce appropriately scaled intermediate variables $\hat{Y}$ and $\hat{H} = \hat{H}(x, \hat{Y})$ defined by

$$y = (cx)^n - \delta\hat{Y}, \quad h = \delta^{\frac{1}{A-B+1}}\hat{H}. \tag{119}$$

At leading order in δ, equation (114) becomes

$$(\hat{H}_{\hat{Y}\hat{Y}} - \hat{H})_{\hat{Y}} + \frac{3\mathcal{F}nc}{\rho g \cos\alpha}(cx)^{n-1}\hat{H}^{B-A} = K\hat{H}^{-A}, \tag{120}$$

whose solutions match with the intermediate limit of the inner solution as $\hat{Y} \to 0^+$ and the intermediate limit of the outer solution as $\hat{Y} \to \infty$.

6 Conclusions

In this paper we obtained similarity solutions that describe the flow of a slender non-uniform rivulet of non-Newtonian power-law fluid down an inclined plane. Rivulets driven by either gravity or a constant shear stress at the free surface were investigated, and in both cases solutions were obtained for both weak and strong surface-tension effects. We found that, despite the rather different physical mechanisms driving the flow, the solutions for gravity-driven and shear-stress-driven rivulets are qualitatively similar. We also found that the similarity exponents m and n are relatively insensitive to the value of the power-law index N for gravity-driven rivulets and independent of N for shear-stress-driven rivulets.

For both driving mechanisms we found that $0 < n < 1$ and $m < 0$ and so solutions with $c > 0$ represent diverging and thinning rivulets in $x > 0$ and solutions with $c < 0$ represent converging and thickening rivulets in $x < 0$. When surface-tension effects are weak there is a unique similarity solution in which the transverse rivulet profile has a single global maximum at $y = 0$. Since c and $\cos\alpha$ must have the same sign solutions with $c > 0$ correspond to sessile rivulets and those with $c < 0$ correspond to pendent rivulets. When surface-tension effects are strong there is a one-parameter family of similarity solutions parameterised by $G_0 = G(0)$ whose behaviour is qualitatively similar for both driving mechanisms. When $c > 0$ the transverse rivulet profile always has a single global maximum at $y = 0$. Solutions are possible only for $G_0 > G_{0c}$ and fail via $G'(1) = 0$ at $G_0 = G_{0c}$. When $c < 0$ solutions are possible for all values of $G_0 \geq 0$ and fail via $G_0 = 0$. The transverse rivulet profile always satisfies $G'(1) < 0$ and has a global maximum at $y = 0$ for $G_0 \geq G_0^*$ and a local minimum at $\eta = 0$ together with two equal global maxima $G = G_m(G_0)$ at $\eta = \pm\eta_m(G_0)$ for $G_0 < G_0^*$.

We also showed how the present similarity solutions can be modified to accommodate a fixed-contact-angle condition at the contact line by incorporating sufficiently strong slip at the solid/fluid interface into the model. Specifically, for gravity-driven rivulets the slip-law exponent M must satisfy $M > (1-N)/N$, while for shear-stress-driven rivulets it must satisfy $M > 0$. The interesting question as to whether or not this procedure selects a unique value of G_0 (or perhaps a range of possible values of G_0) remains open.

Acknowledgements

The first author (SKW) gratefully acknowledges the ongoing financial support of the Leverhulme Trust via a Research Fellowship. The first author also acknowledges the financial support of the City of Paris who funded his stay as a Visiting Professor at the Ecole Superieure de Physique et de Chemie Industrielles de la Ville de Paris during June 2000 where he benefited greatly from discussions with Dr Laurent Limat and his colleagues.

References

[1] P. C. Smith, A similarity solution for slow viscous flow down an inclined plane, *J. Fluid Mech.* **58** (1973) 275–288.

[2] L. W. Schwartz and E. E. Michaelides, Gravity flow of a viscous liquid down a slope with injection, *Phys. Fluids* **31** (1988) 2739–2741.

[3] B. R. Duffy and H. K. Moffatt, A similarity solution for viscous source flow on a vertical plane, *Euro. J. Appl. Math.* **8** (1997) 37–47.

[4] S. K. Wilson, B. R. Duffy and S. H. Davis, On a slender dry patch in a liquid film draining under gravity down an inclined plane, *Euro. J. Appl. Math.* **12** (2001) 233–252.

[5] P. Coussot and S. Proust, Slow, unconfined spreading of a mudflow, *J. Geophys. Res.* **101** (1996) 25217–25229.

[6] S. D. R. Wilson and S. L. Burgess, The steady, spreading flow of a rivulet of mud, *J. Non-Newt. Fluid Mech.* **79** (1998) 77–85.

[7] G. D. Towell and L. B. Rothfeld, Hydrodynamics of rivulet flow, *AIChE J.* **12** (1966) 972–980.

[8] S. Rosenblat, Rivulet flow of a viscoelastic liquid, *J. Non-Newt. Fluid Mech.* **13** (1983) 259–277.

[9] S. V. Alekseenko, P. I. Geshev and P. A. Kuibin, Free-boundary fluid flow on an inclined cylinder, *Physics - Doklady* **42** (1997) 269–272.

[10] B. R. Duffy and H. K. Moffatt, Flow of a viscous trickle on a slowly varying incline, *Chem. Eng. J.* **60** (1995) 141–146.

[11] R. F. Allen and C. M. Biggin, Longitudinal flow of a lenticular liquid filament down an inclined plane, *Phys. Fluids* **17** (1974) 287–291.

[12] S. K. Wilson and B. R. Duffy, On the gravity-driven draining of a rivulet of viscous fluid down a slowly varying substrate with variation transverse to the direction of flow, *Phys. Fluids* **10** (1998) 13–22.

[13] D. Holland, B. R. Duffy and S. K. Wilson, Thermocapillary effects on a thin viscous rivulet draining steadily down a uniformly heated or cooled slowly varying substrate, *J. Fluid Mech.* **441** (2001) 195–221.

[14] S. K. Wilson, B. R. Duffy and A. B. Ross, On the gravity-driven draining of a rivulet of viscoplastic material down a slowly varying substrate, to appear in *Phys. Fluids.*

[15] J. A. Moriarty, L. W. Schwartz and E. O. Tuck, Unsteady spreading of thin liquid films with small surface tension, *Phys. Fluids A* **3** (1991) 733–742.

[16] A. C. King, E. O. Tuck and J.-M. Vanden-Broeck, Air-blown waves on thin viscous sheets, *Phys. Fluids A* **5** (1993) 973–978.

[17] A. C. King and E. O. Tuck, Thin liquid layers supported by steady air-flow surface traction, *J. Fluid Mech.* **251** (1993) 709–718.

[18] T. G. Myers and C. P. Thompson, Modeling the flow of water on aircraft in icing conditions, *A. I. A. A. J.* **36** (1998) 1010–1013.

[19] I. S. McKinley, S. K. Wilson and B. R. Duffy, Spin coating and air-jet blowing of thin viscous drops, *Phys. Fluids* **11** (1999) 30–47.

[20] I. S. McKinley and S. K. Wilson, The linear stability of a ridge of fluid subject to a jet of air, *Phys. Fluids* **13** (2001) 872–883.

[21] I. S. McKinley and S. K. Wilson, The linear stability of a drop of fluid during spin coating or subject to a jet of air, to appear in *Phys. Fluids.*

[22] L. M. Hocking, Sliding and spreading of thin two-dimensional drops, *Q. J. Mech. Appl. Math.* **34** (1981) 37–55.

[23] H. P. Greenspan, On the motion of a small viscous droplet that wets a surface, *J. Fluid Mech.* **84** (1978) 125–143.

Appendix

In this appendix we analyse the asymptotic behaviour of the integral $I = I(G_0, N)$ given by (86) that arises in the solution for a gravity-driven rivulet with strong surface tension, namely

$$I = \int_{-1}^{+1} G^{\frac{2N+1}{N}} \, \mathrm{d}\eta, \quad \text{where} \quad G = (1-\eta^2)\left(G_0 - \frac{S\eta^2}{24}\right), \tag{121}$$

in the strongly shear-thinning limit $N \to 0$.

When $S = 1$ or when $S = -1$ and $G_0 > G_0^*$ the function G has a single global maximum at $\eta = 0$, and as $N \to 0$ the integral in (121) is dominated by the contribution from a narrow "spike" of height $G_0^{(2N+1)/N}$ and semi-width $O(\sqrt{N})$ centered on $\eta = 0$. Thus we define a new variable of integration t_1 by $\eta = \sqrt{N} t_1$ in terms of which (121) can be written

$$I = \sqrt{N} \int_{-\frac{1}{\sqrt{N}}}^{+\frac{1}{\sqrt{N}}} \left[(1 - N t_1^2) \left(G_0 - \frac{S N t_1^2}{24} \right) \right]^{\frac{2N+1}{N}} \mathrm{d}t_1, \tag{122}$$

so that

$$I \sim \sqrt{N} G_0^{\frac{2N+1}{N}} \int_{-\infty}^{+\infty} \left[1 - \left(\frac{S + 24 G_0}{24 G_0} \right) N t_1^2 \right]^{\frac{1}{N}} \mathrm{d}t_1. \tag{123}$$

Since for any X

$$\lim_{N \to 0} (1 + NX)^{\frac{1}{N}} = \exp(X) \tag{124}$$

we have

$$I \sim \sqrt{N} G_0^{\frac{2N+1}{N}} \int_{-\infty}^{+\infty} \exp\left[- \left(\frac{S + 24 G_0}{24 G_0} \right) t_1^2 \right] \mathrm{d}t_1 = 2 G_0^{\frac{5N+2}{2N}} \left[\frac{6\pi N}{S + 24 G_0} \right]^{\frac{1}{2}} \tag{125}$$

as $N \to 0$.

When $S = -1$ and $G_0 = G_0^* = 1/24$ the function $G = (1 - \eta^4)/24$ again has a single global maximum at $\eta = 0$, but as $N \to 0$ the spike that dominates the integral in (121) has semi-width $O(N^{1/4})$ rather than $O(\sqrt{N})$. Thus we define a new variable of integration t_2 by $\eta = N^{1/4} t_2$ in terms of which (121) can be written

$$I = N^{\frac{1}{4}} \left(\frac{1}{24} \right)^{\frac{2N+1}{N}} \int_{-N^{-\frac{1}{4}}}^{+N^{-\frac{1}{4}}} (1 - N t_2^4)^{\frac{2N+1}{N}} \mathrm{d}t_2, \tag{126}$$

so that

$$I \sim N^{\frac{1}{4}} \left(\frac{1}{24} \right)^{\frac{2N+1}{N}} \int_{-\infty}^{+\infty} (1 - N t_2^4)^{\frac{1}{N}} \mathrm{d}t_2, \tag{127}$$

and hence using (124)

$$I \sim N^{\frac{1}{4}} \left(\frac{1}{24} \right)^{\frac{2N+1}{N}} \int_{-\infty}^{+\infty} \exp(-t_2^4) \, \mathrm{d}t_2 = \frac{1}{2} \left(\frac{1}{24} \right)^{\frac{2N+1}{N}} N^{\frac{1}{4}} \Gamma\left(\tfrac{1}{4} \right) \tag{128}$$

as $N \to 0$.

When $S = -1$ and $G_0 < G_0^*$ the function G has two global maxima $G = G_\mathrm{m}$ at $\eta = \pm \eta_\mathrm{m}$, where G_m and η_m are given by (88), and as $N \to 0$ the integral in (121) is dominated by the contributions from two narrow spikes of height $G_\mathrm{m}^{(2N+1)/N}$ and semi-width $O(\sqrt{N})$ centered on $\eta = \pm \eta_\mathrm{m}$. Thus we define a new variable of integration t_3 by $\eta = \eta_\mathrm{m} + \sqrt{N} t_3$ in terms of which (121) can be written

$$I = 2\sqrt{N} \int_{-\frac{\eta_\mathrm{m}}{\sqrt{N}}}^{+\frac{1-\eta_\mathrm{m}}{\sqrt{N}}} \left[(1 - (\eta_\mathrm{m} + \sqrt{N} t_3)^2) \left(G_0 + \frac{(\eta_\mathrm{m} + \sqrt{N} t_3)^2}{24} \right) \right]^{\frac{2N+1}{N}} \mathrm{d}t_3, \tag{129}$$

so that

$$I \sim 2\sqrt{N} G_{\mathrm{m}}^{\frac{2N+1}{N}} \int_{-\infty}^{+\infty} \left[1 - \left(\frac{1-24G_0}{12G_{\mathrm{m}}}\right) N t_3^2\right]^{\frac{1}{N}} \mathrm{d}t_3, \tag{130}$$

and hence using (124)

$$I \sim 2\sqrt{N} G_{\mathrm{m}}^{\frac{2N+1}{N}} \int_{-\infty}^{+\infty} \exp\left[-\left(\frac{1-24G_0}{12G_{\mathrm{m}}}\right) t_3^2\right] \mathrm{d}t_3 = 4 G_{\mathrm{m}}^{\frac{5N+2}{2N}} \left[\frac{3\pi N}{1-24G_0}\right]^{\frac{1}{2}} \tag{131}$$

as $N \to 0$.

The results (125), (128) and (131) are the ones quoted in (90).

Figure Captions

FIGURE 1 : Geometry of the problem.

FIGURE 2 : The integral $I = I(N)$ given by (54) for a gravity-driven rivulet with weak surface tension plotted as a function of N.

FIGURE 3 : Transverse rivulet profiles $G = G(\eta)$ given by (84) for a gravity-driven rivulet with strong surface tension plotted as a function of η when (a) $S = 1$ for $G_0 = G_{0c} = 1/24$, $1/12$, $1/8$ and $1/6$, and (b) $S = -1$ for $G_0 = 0$, $1/48$, $G_0^* = 1/24$, $1/16$ and $1/12$.

FIGURE 4 : The integral $I = I(G_0, N)$ given by (86) for a gravity-driven rivulet with strong surface tension plotted as (a) a function of G_0 for a range of values of N for both $S = 1$ and $S = -1$, and (b) a function of N for $G_0 = 0.1$, 0.2, ..., 1.2 for both $S = 1$ and $S = -1$. For clarity in part (b) values for $S = 1$ are denoted with a solid line and those for $S = -1$ with a dashed line.

FIGURE 5 : Numerically calculated transverse rivulet profiles $G = G(\eta)$ obtained from (101) for a shear-stress-driven rivulet with strong surface tension plotted as a function of η when (a) $S = 1$ for $G_0 = G_{0c} \simeq 0.4277$, 0.8, 1.2 and 1.6, and (b) $S = -1$ for $G_0 = 0$, $G_0^* \simeq 0.2138$, 0.4, 0.8, 1.2 and 1.6.

FIGURE 6 : The integral $I = I(G_0)$ given by (103) for a shear-stress-driven rivulet with strong surface tension plotted as a function of G_0 for both $S = 1$ and $S = -1$.

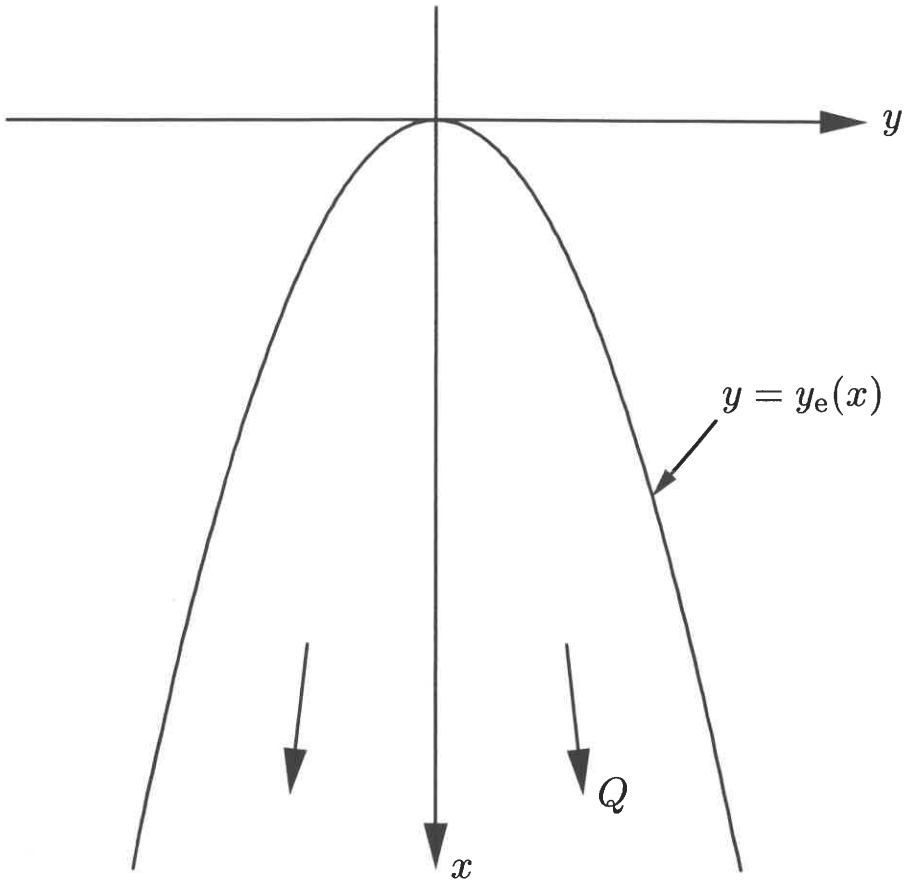

Figure 1

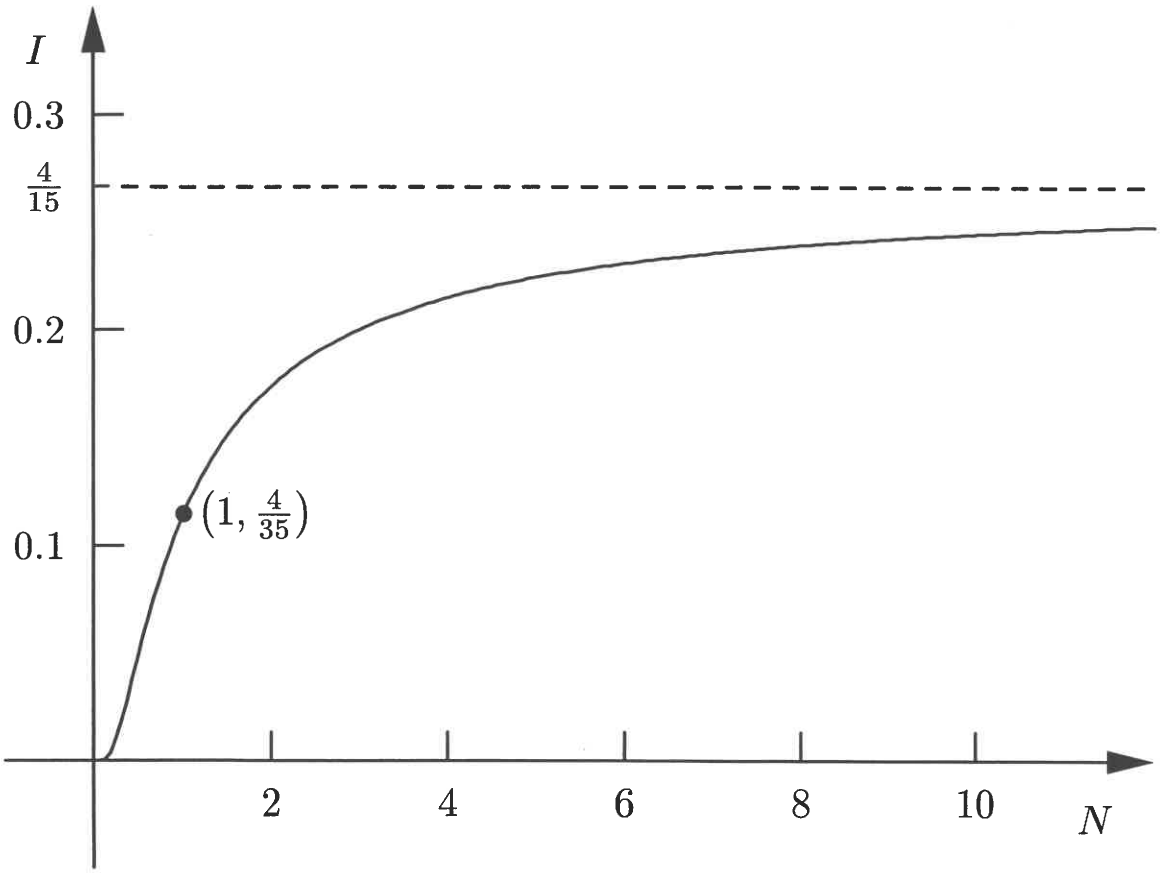

Figure 2

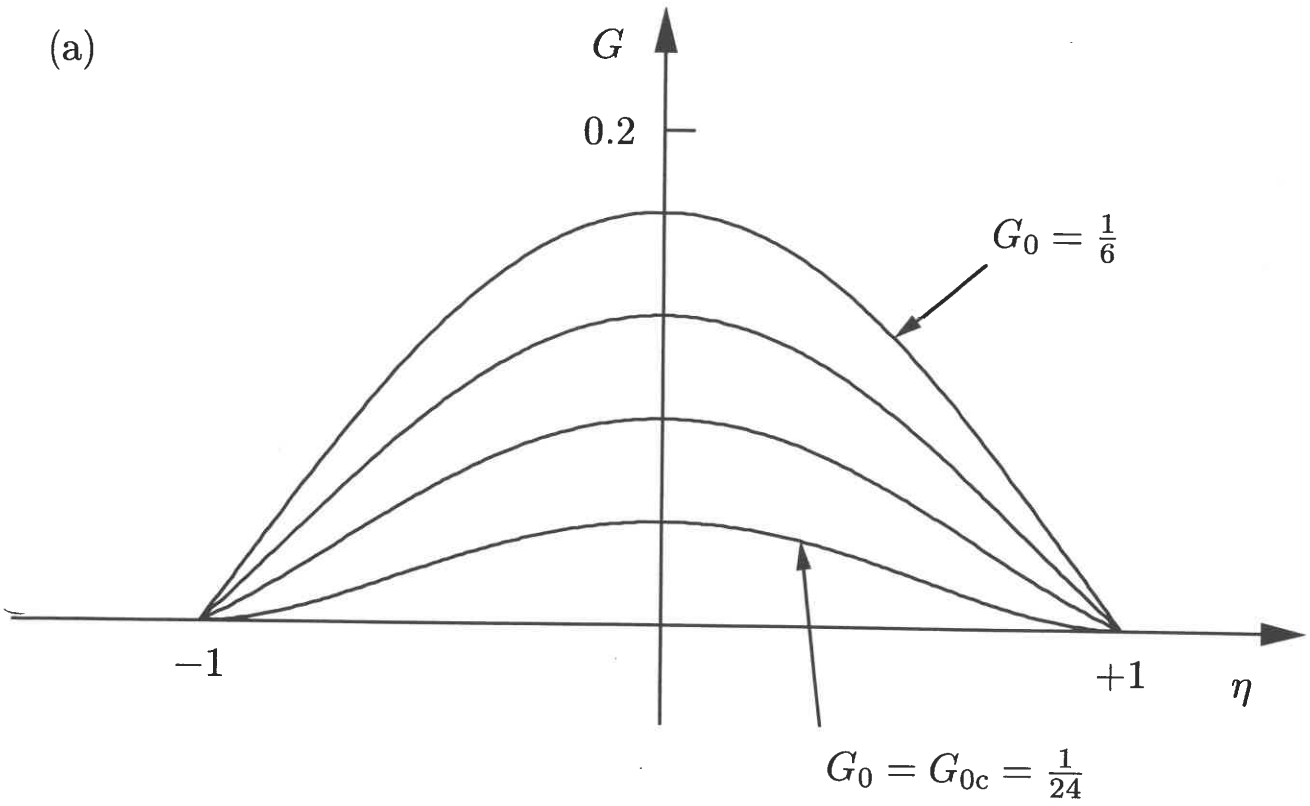
(a)
G
0.2
$G_0 = \frac{1}{6}$
−1
+1
η
$G_0 = G_{0c} = \frac{1}{24}$

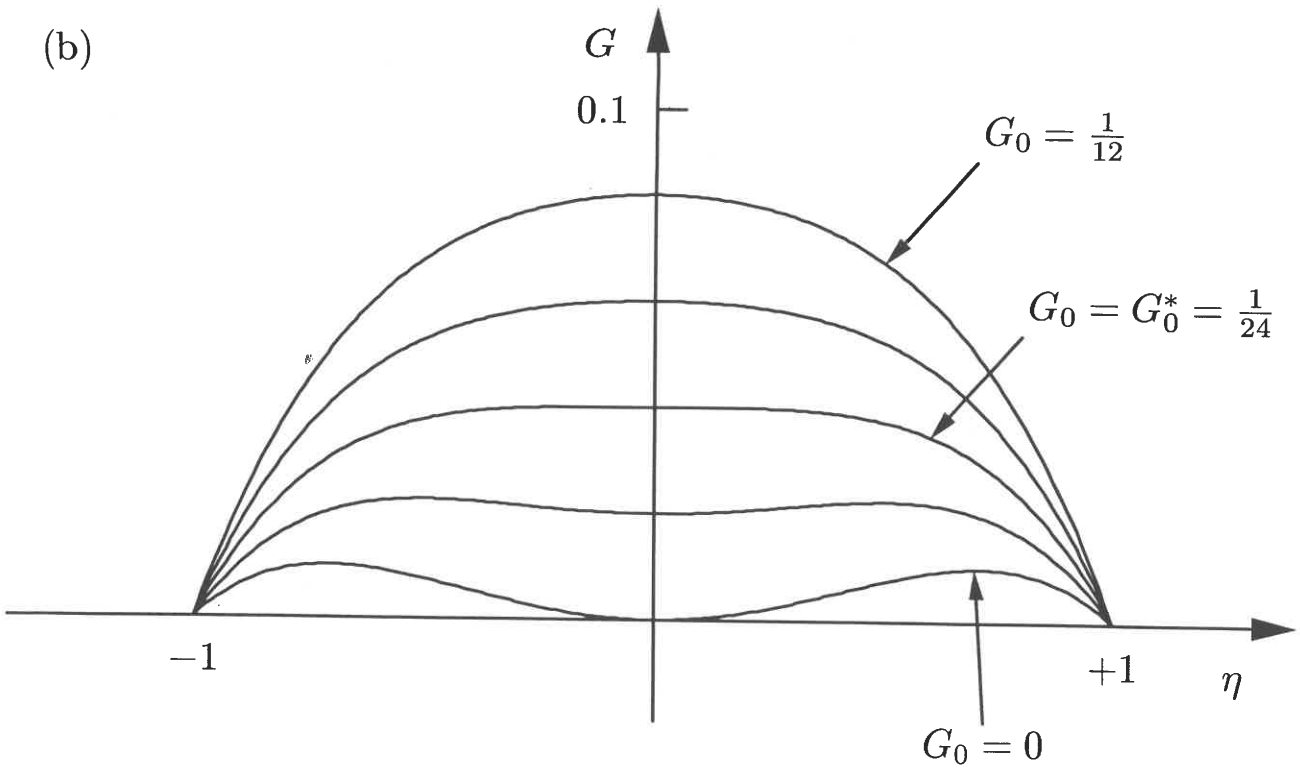
(b)
G
0.1
$G_0 = \frac{1}{12}$
$G_0 = G_0^* = \frac{1}{24}$
−1
+1
η
$G_0 = 0$

Figure 3

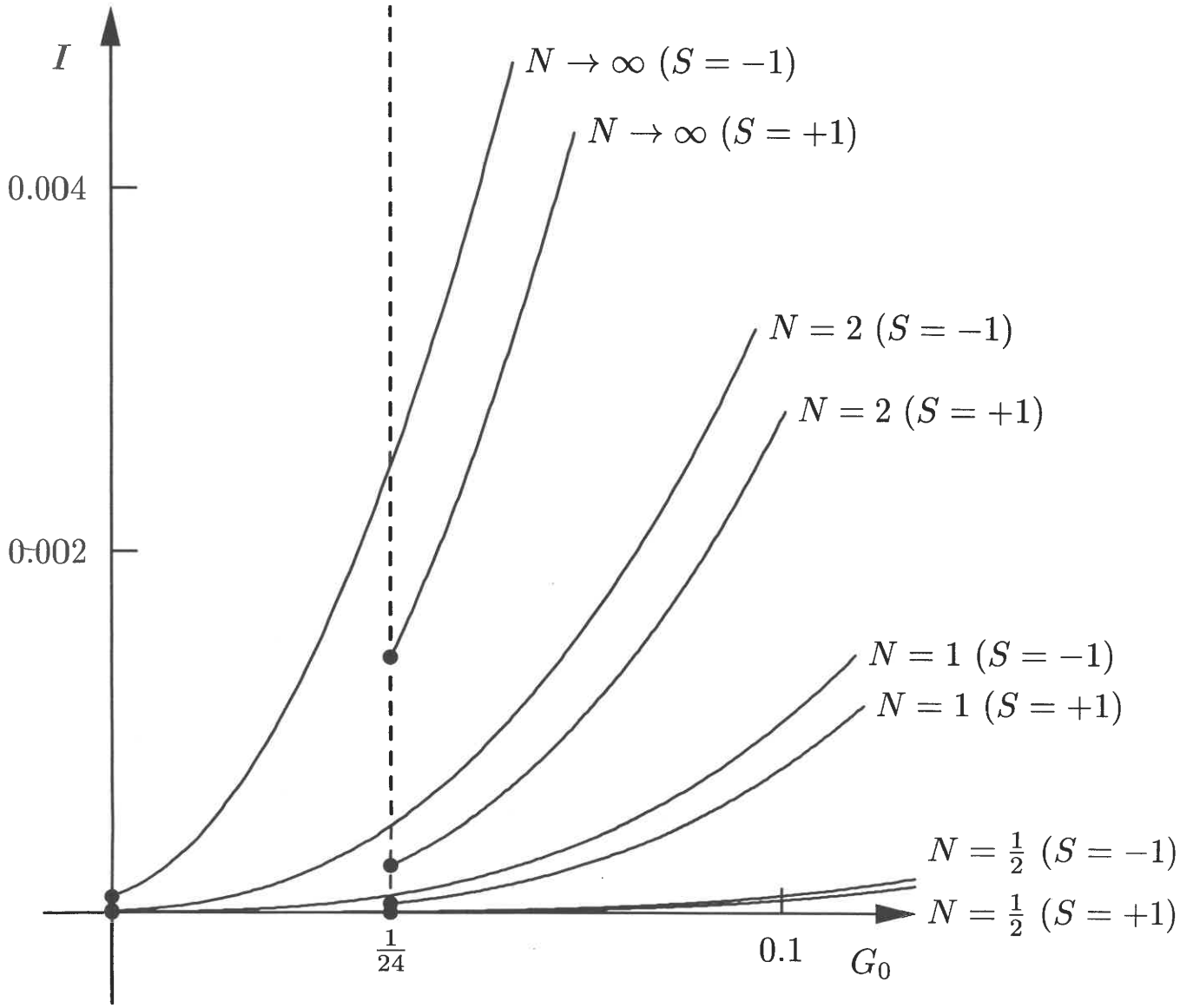
I
0.004
0.002
$N \to \infty$ $(S = -1)$
$N \to \infty$ $(S = +1)$
$N = 2$ $(S = -1)$
$N = 2$ $(S = +1)$
$N = 1$ $(S = -1)$
$N = 1$ $(S = +1)$
$N = \frac{1}{2}$ $(S = -1)$
$N = \frac{1}{2}$ $(S = +1)$
$\frac{1}{24}$
0.1
G_0

Figure 4(a)

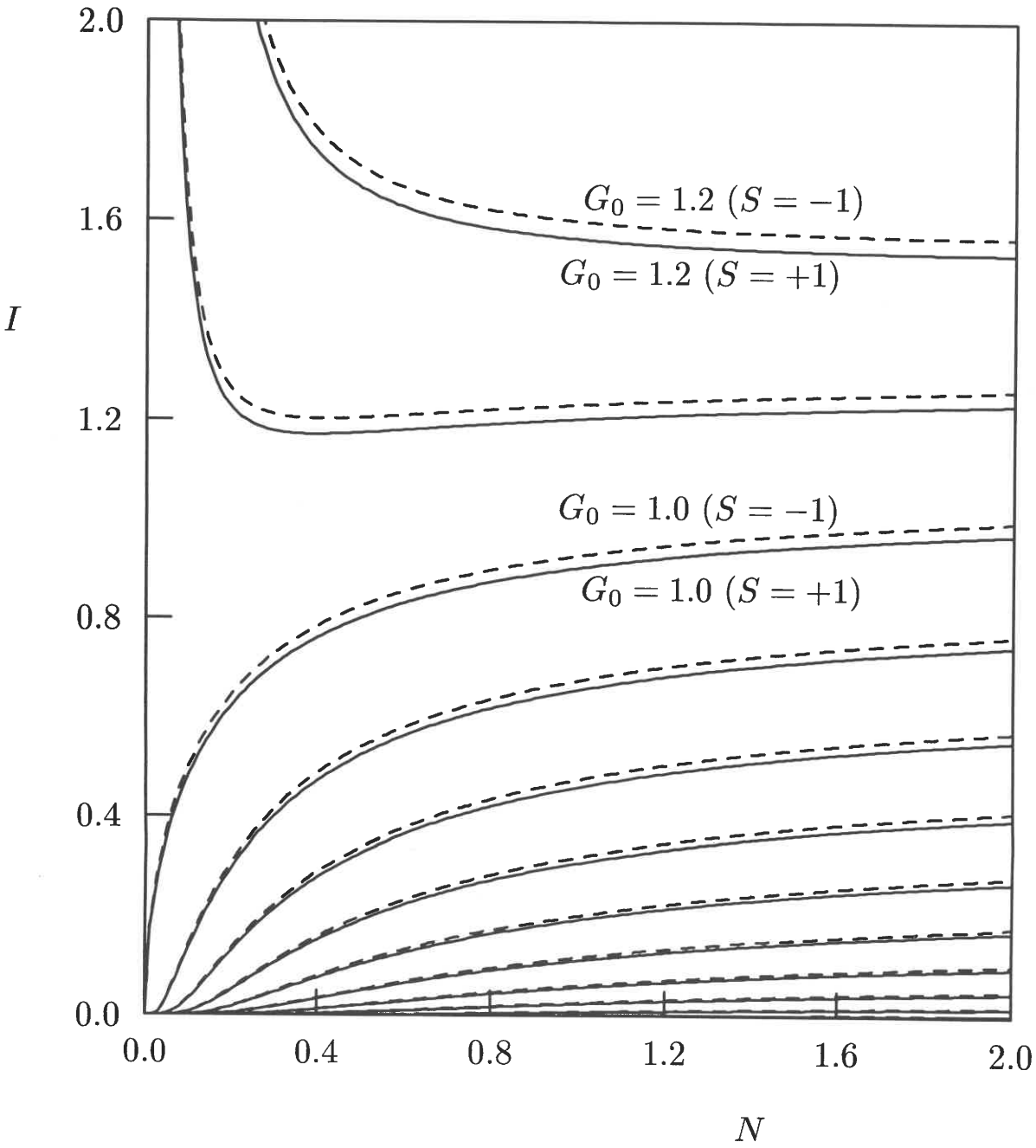
2.0
1.6
1.2
0.8
0.4
0.0
I
$G_0 = 1.2$ $(S = -1)$
$G_0 = 1.2$ $(S = +1)$
$G_0 = 1.0$ $(S = -1)$
$G_0 = 1.0$ $(S = +1)$
0.0
0.4
0.8
1.2
1.6
2.0
N

Figure 4(b)

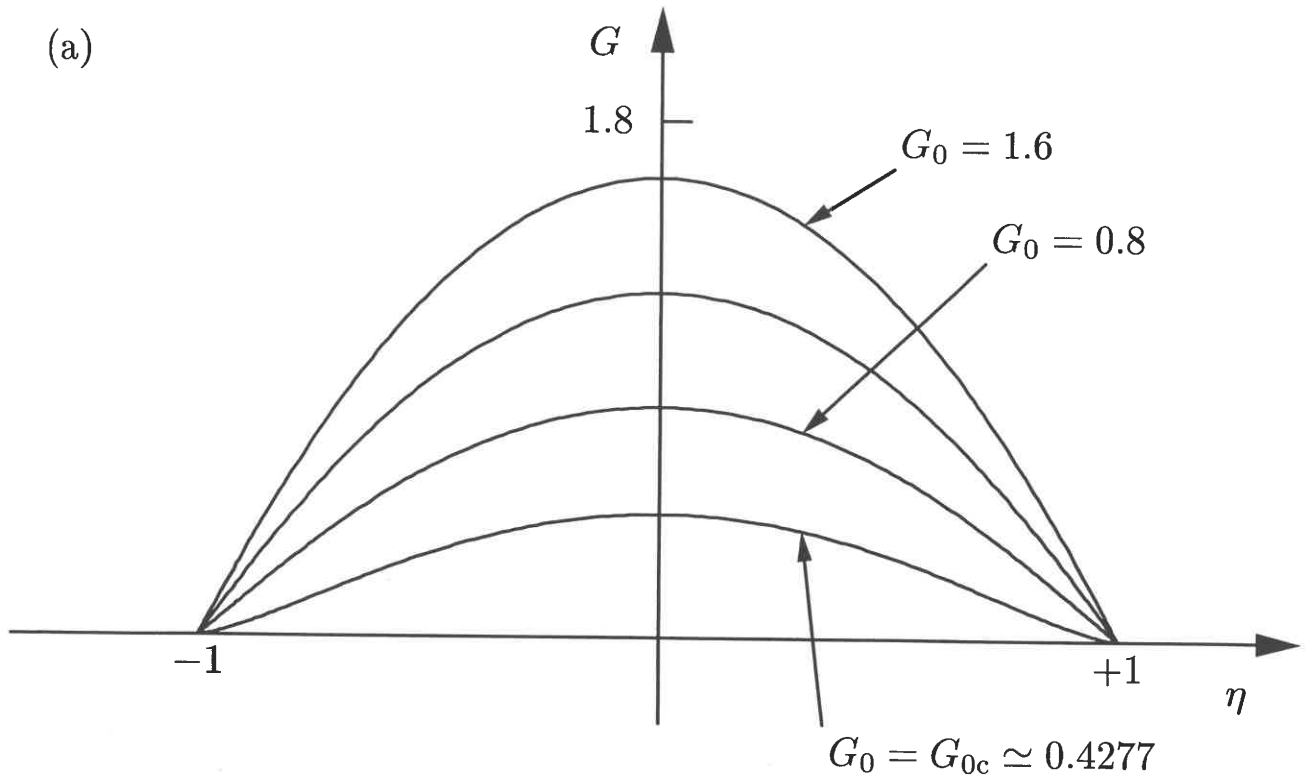
(a)
G
1.8
$G_0 = 1.6$
$G_0 = 0.8$
−1
+1
η
$G_0 = G_{0c} \simeq 0.4277$

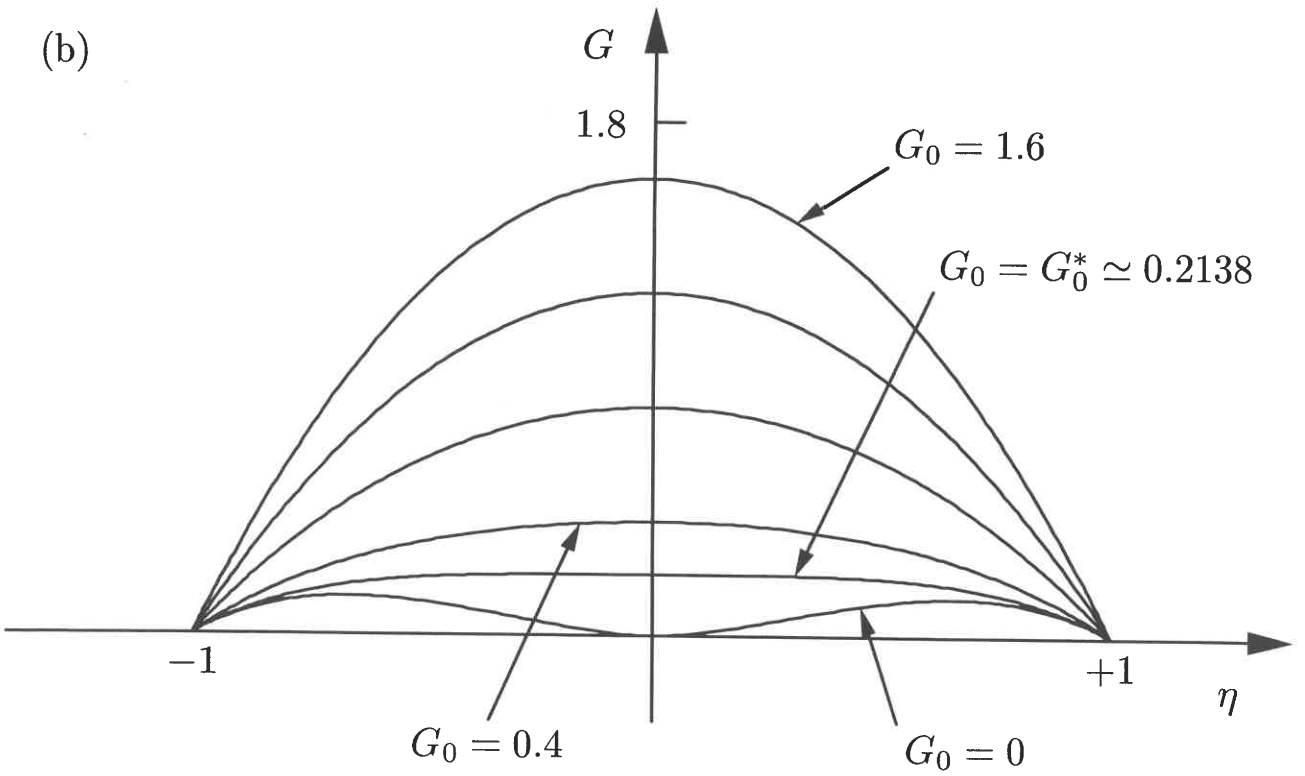
(b)
G
1.8
$G_0 = 1.6$
$G_0 = G_0^* \simeq 0.2138$
−1
+1
η
$G_0 = 0.4$
$G_0 = 0$

Figure 5

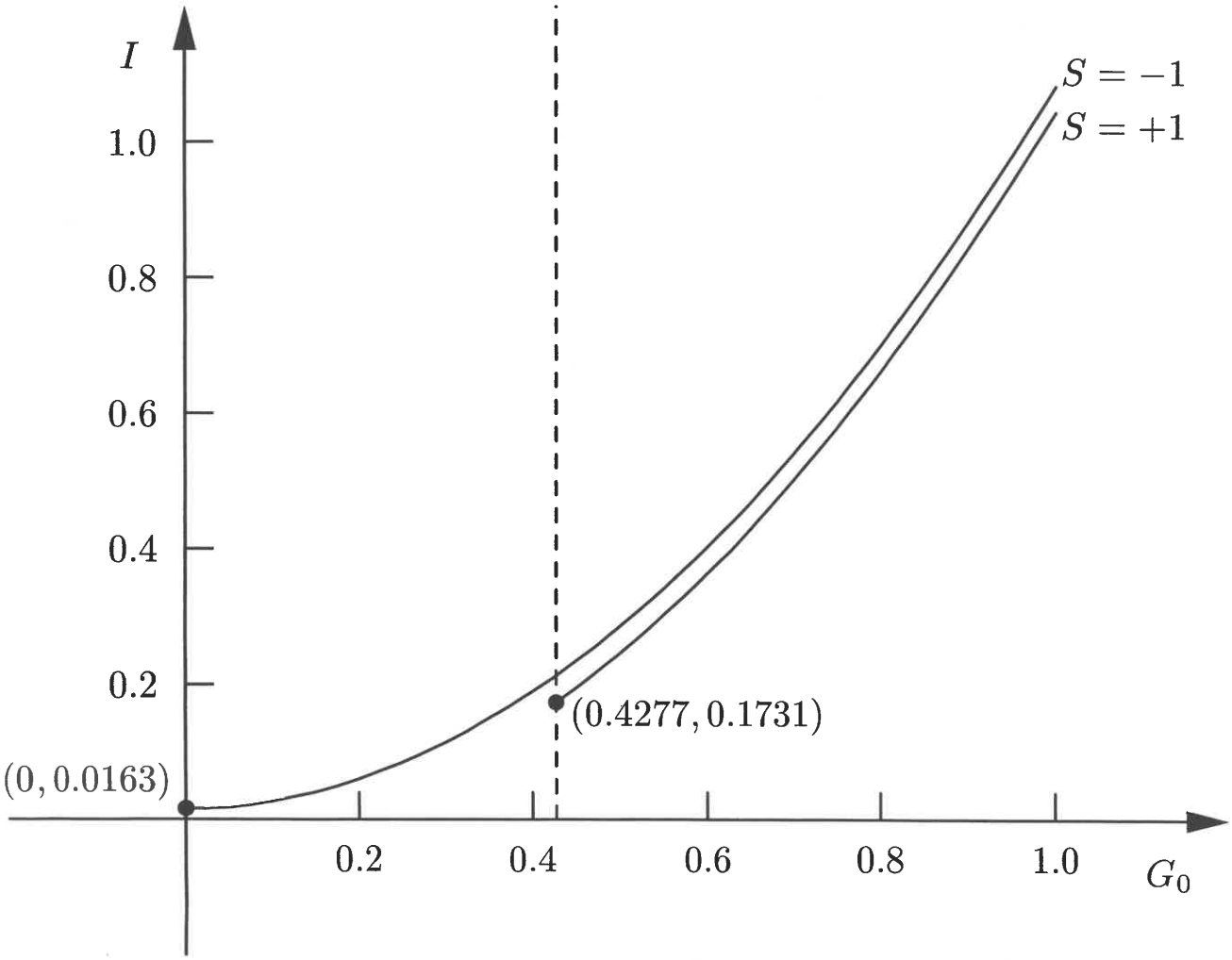

Figure 6